Available online at www.sciencedirect.com

ScienceDirect

Ceramics International 40 (2014) 827–833

CERAMICS INTERNATIONAL

www.elsevier.com/locate/ceramint

Influence of thickness of MgO overlayer on the properties of ZnO thin films prepared on *c*-plane sapphire for H_2 sensing

K. Vijayalakshmi[a,*], K. Karthick[a], P. Deepak Raj[b], M. Sridharan[b]

[a]*Research Department of Physics, Bishop Heber College, Tiruchirapalli 620017, India*

[b]*Functional Nanomaterials and Devices Lab, Centre for Nanotechnology and Advanced Biomaterials and School of Electrical and Electronics Engineering, SASTRA University, Thanjavur 613401, India*

Received 11 June 2013; received in revised form 20 June 2013; accepted 20 June 2013
Available online 28 June 2013

Abstract

ZnO/MgO double layered thin films were prepared on Al_2O_3 substrate by direct current (dc) sputtering at a low power of 40 W. The effect of thickness of MgO overlayer on the properties of ZnO films was investigated. X-ray diffraction patterns revealed that the crystallinity of ZnO films can be improved by addition of a MgO overlayer. The blueshift in the PL peak suggests that the optical bandgap of ZnO can be tuned by varying the thickness of MgO overlayer. SEM micrographs revealed that the surface morphology changes from uniform to dense porous and nano-flake like structure with increase in thickness of MgO layer. Pure ZnO and optimized ZnO/MgO films were tested for their sensing performance towards H_2 at different temperatures. The maximum response of ZnO and ZnO/MgO sensor was observed to be 135 and 260, respectively, at an operating temperature of 140 °C. The very high sensitivity at such a low operating temperature is associated with the fast recovery time of 120 s, which could be achieved due to the promoting effect of MgO on ZnO.

Keywords: Thin films; Sputtering; SEM; H_2 sensors

1. Introduction

Hydrogen (H_2) gas is emerging as one of the most useful gases especially as a fuel in recent years. It is highly flammable in air with lower flammability limit of 4.65% beyond which it easily catches fire. Hence, detection of H_2 gas leakage becomes extremely important to prevent accidents in the environment. The main effort of H_2 sensor development has been the improvement of H_2 gas sensitivity as well as selectivity and to decrease the operating temperature. Hence, compact, reliable, and low power consumption sensor devices that can detect hydrogen have been the subject of many research groups [1–3]. Semiconductor metal oxide sensors were studied and used extensively for hydrogen detection for their simplicity, reliability and low cost [4]. Among several metal oxide semiconductors, zinc oxide (ZnO) is one of the most promising and useful material for chemical gas sensor devices, due to its attractive properties such as wide bandgap (3.3 eV at room temperature) and large exciton binding energy (60 meV). The physical properties of ZnO depend on the microstructure of the material, including crystal size, morphology and orientation [5,6]. Sensing properties of ZnO are directly related to its preparation history, particle size, morphology and operating temperature. However, it still remains a challenge to enhance their performance and detection limit. Various techniques have been developed to improve the sensitivity of ZnO based sensors such as doping, surface coating and fabrication of heterostructures. Among these technologies, surface coating of ZnO with metal oxides may be the most effective technique, because the optical properties of ZnO coated with a MgO layer can change upon exposure to gas and can be restored upon reexposure in air even at room temperature [7]. Such low temperature processes are very desirable in the detection of H_2 gas. Magnesium oxide (MgO) is the best candidate to be used as overlayer due to its excellent properties such as large bandgap (7.5 eV) and optical transparency. Because of the similarity in atomic radii, MgO has the ability to tune the bandgap of ZnO without affecting the lattice constant. Bandgap enhancement of ZnO by doping

*Corresponding author. Tel.: +91 9994647287.
E-mail address: viji71naveen@yahoo.com (K. Vijayalakshmi).

0272-8842/$ - see front matter © 2013 Elsevier Ltd and Techna Group S.r.l. All rights reserved.
http://dx.doi.org/10.1016/j.ceramint.2013.06.075

Mg, without altering the ZnO structure has been reported widely [8]. However, studies on the effect of varying thickness of the MgO overlayer on ZnO for bandgap modulation have not been reported widely. Besides this, to the best of our knowledge, there has been no report on H_2 sensing properties of ZnO/MgO bilayer films.

Several deposition techniques are used to prepare ZnO/MgO thin films such as sputtering, pulsed laser deposition, sol–gel method, solid state synthesis method and plasma assisted molecular beam epitaxy [9–13]. Among these techniques, dc sputtering is one of the convenient methods for preparing buffer layer of metal oxide semiconducting thin films. It has several advantages, such as large area deposition, strong adhesion, excellent uniformity, purity with high density, and nanophase. In this article, we report the deposition of ZnO/MgO double layered films on sapphire substrate at low sputtering power, with substrate at room temperature. The influences of thickness of MgO overlayer on the crystallization, morphology and energy bandgap of ZnO films were investigated. The response of optimized ZnO/MgO sensors towards H_2 was compared with that of the pure ZnO sensor.

2. Experimental details

The preparation of MgO/ZnO films was carried out by dc magnetron sputtering. ZnO thin films were deposited on 0.3 mm thick *c*-cut (Al_2O_3) sapphire substrate at room temperature using a zinc (99.999% purity Sigma Aldrich) metal target of 2 in. diameter. Before deposition, the substrates were cleaned in acetone and ethanol for 15 min, and rinsed in ultra-pure water for removal of impurities over the substrates. The cleaned substrate was loaded in the sputtering chamber with the target to the substrate distance fixed at 400 mm. The chamber was initially evacuated to a base pressure of 10^{-5} Pa and sustained at 10^{-1} Pa during film deposition. A mixture of oxygen and argon with high purity in the ratio of 1:2 was used as the sputtering gas. ZnO film was deposited for a constant duration of 30 min with a low dc power of 40 W. After the deposition of ZnO film, a overlayer of MgO was deposited onto the surface of oxide film. The MgO overlayer was sputtered using a Mg metal target of 2 in. diameter at the same power of 40 W. The thickness of the sputtered MgO overlayer is varied from 275 to 325 nm to study its influence on the properties of ZnO thin films. The resultant films were further used to investigate the phase orientation, optical, photoluminescence and morphological properties. The structural characterization of the films was carried out by an X'Perto X-ray diffractometer and optical characterization using a UV–vis Lambda-35 spectrophotometer over the wavelength range of 350–850 nm. Photoluminescence (PL) studies were performed using a Varian Carry Eclipse PL spectrophotometer. SEM analyses of the ZnO/MgO films were carried using a HITACHI high technologies SU9000 UHRE field emission scanning electron microscope. The ZnO/MgO films prepared under the best deposition conditions found were used to fabricate a H_2 gas sensor. Fig. 1 shows a schematic diagram of the experimental set-up used for measuring the sensor response. The H_2 and N_2 gases were admitted inside the chamber using separate mass flow controllers. The response of the sensor for reducing gases was determined using the relation [14] $S = Ra/Rg$, where Ra and Rg are the electrical resistance of the sensor in the presence of air and in test gas, respectively.

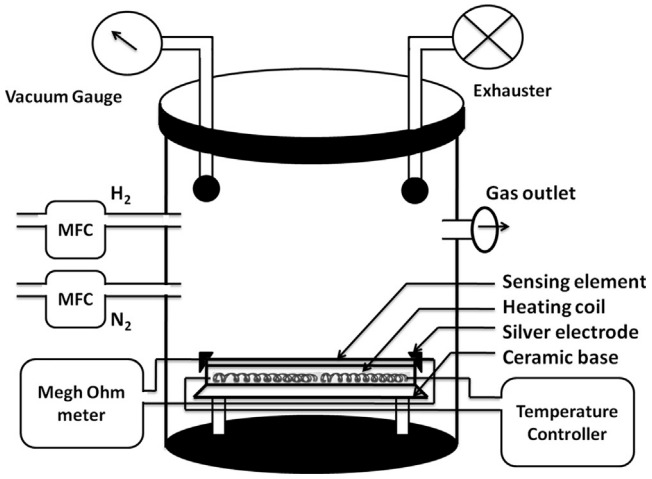

Fig. 1. Schematic diagram of the gas sensor measuring system.

3. Results and discussion

3.1. Effect of MgO overlayer on the structural properties of ZnO film

Fig. 2 shows the XRD patterns of ZnO film deposited on Al_2O_3 (0001) sapphire substrate for different thicknesses of MgO overlayer. As predicted, no extra peak other than the preferentially orientated (002) peak from ZnO and (200) peak from MgO is obtained. Due to the underlayer of ZnO, the (200) peak of MgO is perpendicular to the surface of the substrate. The intensity of (002) peak significantly increased with MgO overlayer up to a thickness of 275 nm, which suggests that the crystalline quality and *c*-axis orientation of the films can be enhanced by the diffusion of Mg^{2+} ions into ZnO lattice. This implies that the energy contribution of Mg ions to zinc is maximum at the thickness of 275 nm in contrast to those of the other ZnO/MgO samples. In addition, the intensity of MgO (200) peak decreased with increase in thickness of MgO layer with a minimum at 275 nm. This may be attributed to the presence of more unreacted Mg atoms in the case of ZnO films with 175 and 225 nm thick MgO layer, while for 275 nm layer there are only fewer unreacted atoms, leading to better crystallite quality of the films. There is no shift in the peak along the *c*-plane of ZnO, indicating the diffusion of Mg^{2+} ions without affecting the phase orientation. When Mg ions diffuse into ZnO lattice there is no chance for adverse effect by the substrate, because it is maintained at room temperature. For 325 nm thick MgO layer, ZnO peak intensity decreased, while the MgO peak intensity increased, indicating the decreased oxygen adsorption in the lattice sites leading to the deterioration of crystallinity and preferred orientation at higher thickness. The mean crystallite size (*D*)

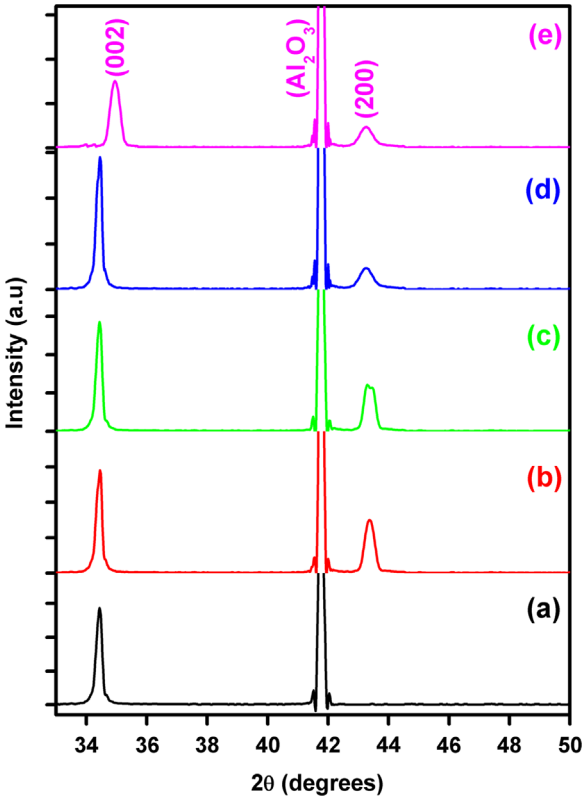

Fig. 2. XRD patterns of ZnO films with different thicknesses of MgO overlayer: (a) pure ZnO, (b) ZnO/MgO (175 nm), (c) ZnO/MgO (225 nm), (d) ZnO/MgO (275 nm), and (e) ZnO/MgO (325 nm).

Table 1
Structural parameters of ZnO/MgO films for different thicknesses of MgO overlayer.

Thickness of MgO layer (nm)	Crystallite size (nm)	Lattice constant c (Å)
175	28	5.27
225	23	5.25
275	18	5.12
325	22	5.23

of ZnO and ZnO/MgO films was estimated using Debye–Scherrer's formula [15]

$$D = K\lambda/\beta\cos\theta \quad (1)$$

where k is the shape factor of the average crystallite (0.91), λ is the X-ray wavelength ($\lambda = 0.15406$ nm), β is the full width at half-maximum (FWHM) in radians and θ is the Bragg angle.

The c-axis lattice constant was calculated using the following expression [16]:

$$\frac{1}{d_{hkl}^2} = \frac{4}{3}\left[\frac{h^2 + hk + k^2}{a^2}\right] + \frac{l^2}{c^2} \quad (2)$$

The values of crystallite size (D) and c-axis lattice constant for ZnO and ZnO/MgO films are listed in Table 1. The results revealed that the c-axis length is decreased with MgO layer, which confirms the incorporation of Mg ions into ZnO lattice, because the ionic radius of Mg^{2+} (0.057 nm) is slightly smaller

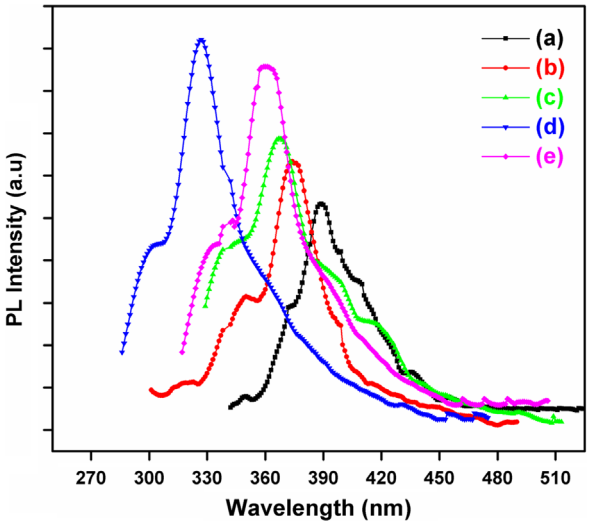

Fig. 3. Photoluminescence spectra of ZnO films with different thicknesses of MgO overlayer: (a) pure ZnO, (b) ZnO/MgO (175 nm), (c) ZnO/MgO (225 nm), (d) ZnO/MgO (275 nm), and (e) ZnO/MgO (325 nm).

than that of Zn^{2+} (0.060 nm). Chen et al. reported that the Mg^{2+} incorporation into ZnO lattice causes the decrease of the c-axis length [17].

3.2. Effect of MgO overlayer on the luminescence properties of ZnO film

The luminescence property provides information on the optically active defects and relaxation pathways of excited states [18]. The room temperature PL spectra of ZnO and ZnO/MgO films are displayed in Fig. 3. From the emission spectra, it is inferred that the near band emission (NBE) in the UV region is at around 385 nm for pure ZnO. Previous reports on PL emission indicate that the UV emission peak usually originates from an NBE transition which is due to exciton related recombination [19]. The diffusion of Mg ions into ZnO lattice induced an increase in NBE peak intensity in ZnO/MgO film. These results suggested that the overlayer of MgO on ZnO is effective in achieving improved optical properties of ZnO. Moreover, the peak intensity of the NBE increased with increase in thickness of MgO layer showing an increase in crystallinity in the sample as revealed from XRD results. In thin films, the non-radiative defect is induced by the crystal imperfections, such as oxygen vacancies, during deposition [20]. These defects suppress the luminescence intensity and induce defect emission. In our case, the PL intensity increased with increase in the thickness of MgO layer due to decrease of the non-radiative defects. Absence of intrinsic host lattice side effects during film deposition is confirmed due to the devoid of defect emission in all samples. As expected, the ultra-emission peak greatly shifted towards lower wavelength side for the thickness of MgO up to 275 nm, because of the modulation of the band-gap focused by the swap of Mg, which suggests that the optical bandgap of the ZnO thin films can be tuned by fabricating MgO overlayer on ZnO. The large shift observed for 275 nm thickness of MgO indicates that such emission may possibly be due to the recombination between the shallow donor and deep acceptor, but

not from the shallow donor related exciton (D^0x). The blueshift in the PL peak confirms the confinement effect due to the overlayer of MgO on ZnO. Further increase in the MgO thickness to 325 nm decreased the PL intensity, and the peak position also shifted towards higher wavelength, indicating the degradation of bandgap enhancement. High crystal quality and the confinement effect related to the nanostructures are the two factors favoring the increase in intensity of UV emission at room temperature. Nanostructured ZnO films exhibit quantum confinement effects [21], and in the present case the increase in thickness of MgO overlayer causes blueshift in photo-absorption due to enhanced quantum confinement effects. Moreover, the bandgap of ZnO in the present ZnO/MgO double layer films exhibits a more pronounced shift with increase in the thickness of MgO, with a very significant increase of about 3.69 eV for 275 nm thick MgO layer. This pronounced effect may be due to large bandgap MgO surface coating that tends to isolate ZnO crystallites and layers from each other for enhanced quantum confinement effects. The pronounced increase with thickness in our double layer films may arise due to the diffusion and adjustments that lead to gradual conversion of 2-D layers into 3-D islands or crystallites by MgO.

3.3. Effect of MgO overlayer on the morphological properties of ZnO film

SE-micrograph provides information on the contour features of the samples, which allow us to inspect the shape, size and diameter of the samples by scanning it with a focused beam of

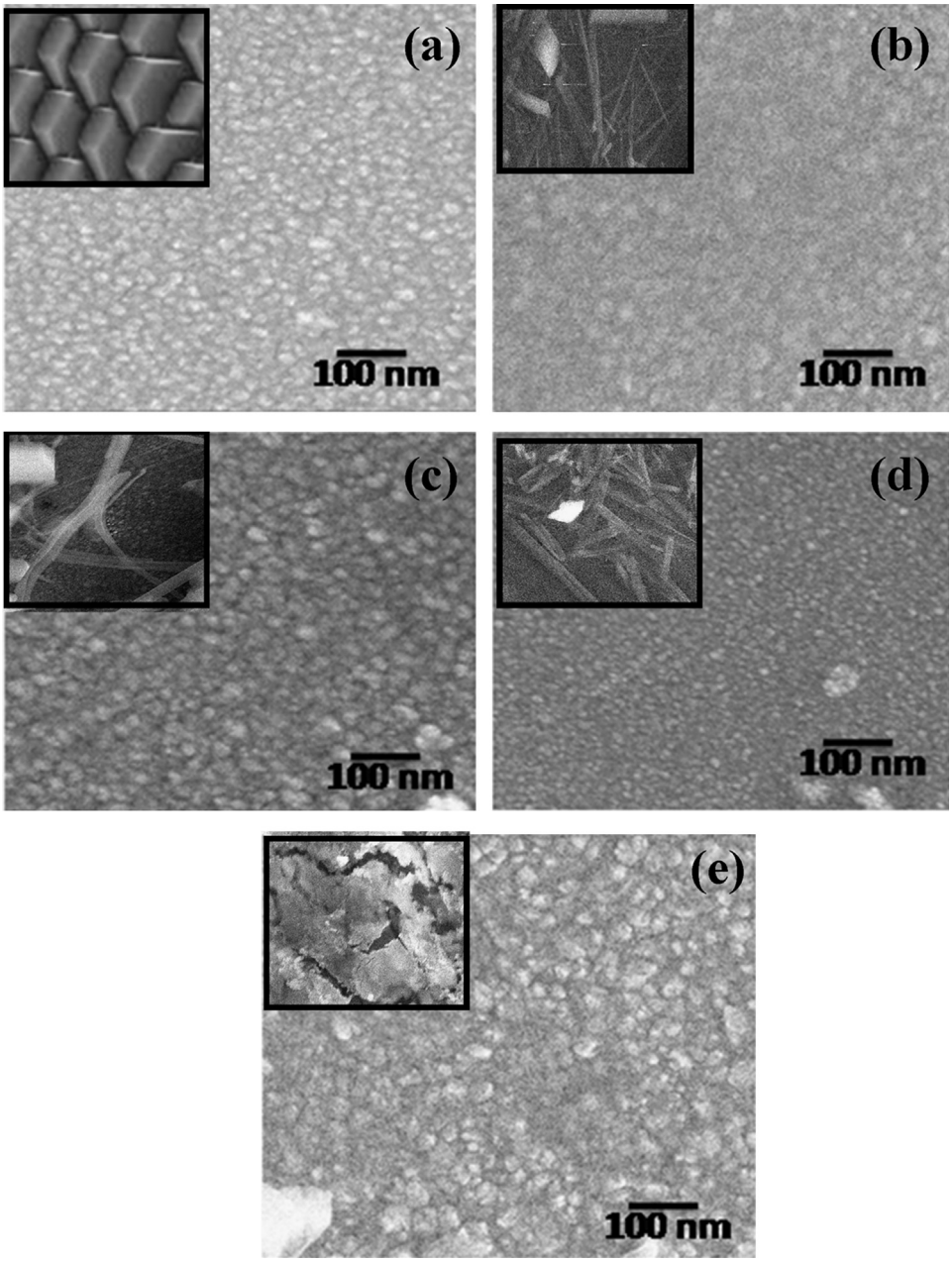

Fig. 4. HRSEM images of ZnO films with different thicknesses of MgO overlayer: (a) pure ZnO, (b) ZnO/MgO (175 nm), (c) ZnO/MgO (225 nm), (d) ZnO/MgO (275 nm), and (e) ZnO/MgO (325 nm).

electrons [22]. In order to study the effect of Mg diffusion on the morphology of ZnO film, FE-SEM analysis was carried out. The SE-micrographs of pure ZnO and ZnO/MgO films with varying thickness of MgO are shown in Fig. 4. The micrograph of pure ZnO film displays a uniform coating throughout the sapphire substrate with hexagonal shaped grains. The micrographs also show that the morphology of the film is greatly influenced by different thicknesses of MgO overlayer on ZnO. Initially, for thin MgO overlayer of 175 nm, the film exhibited random distribution of smaller size particles due to sluggish growth of grains. Few ZnO nanowires are observed in the high magnification image, which is shown as inset in Fig. 4(b). When the thickness of MgO overlayer was increased to 225 nm, dense porous surface with well grown nanowires (inset in Fig. 4(c)) was observed. For 275 nm thick MgO layer, uniform and compact granular morphology with nanoflake like structure (inset in Fig. 4(d)) is observed, due to improvement in the crystallinity of the films. The presence of more number of micropores in the film indicates that it is favorable for sensing application. The micrographs displayed clearly that there is no visible defect over the surface of the film. As expected, with increase in the thickness of MgO, the lattice mismatch between ZnO/MgO films and Al_2O_3 (0001) sapphire is minimum, because the lattice constant value of sapphire (a=4.785 Å, c=12.991 Å) is close to that of Mg (a=4.25 Å). The size of the grains decreases with the MgO layer which confirms that more Mg ions diffuse into ZnO. According to the phase diagram of the ZnO–MgO binary system, the thermodynamic solid solubility of MgO in ZnO is less than 4 mol% [23]. Hence, diffusion of MgO into ZnO with limited solubility leads to decrease in grain size [24]. There is no change in the crystal structure after the surface coverage of ZnO by MgO which is confirmed from the micrographs. At a higher thickness of 375 nm, the dense surface structure disappeared and some cracks are observed on the grains indicating the degradation of the crystalline quality as revealed from XRD results.

3.4. Gas sensing studies

After having optimized the thickness of MgO overlayer on ZnO, a ZnO/MgO sensor device was fabricated with 275 nm thick MgO layer. A schematic representation of the ZnO/MgO sensor device is shown in Fig. 5. The response of pure ZnO, and ZnO/MgO film sensor was studied for its performance towards H_2. Fig. 6 shows the effect of MgO overlayer on the resistance of ZnO and ZnO/MgO films with time, towards 300 sccm of hydrogen at room temperature. It was observed that the resistance decreased when the sensors were exposed to H_2 gas. On the other hand, the resistance retraces back to the initial value when the H_2 supply was stopped. The variation in resistance of ZnO sensors is induced by the adsorption and desorption of O_2 molecules from the surfaces of the grains. In the air environment, O_2 molecules are chemisorbed onto the surface of ZnO as oxygen ions (O_2^-, O^- and O^{2-}) and extract electrons from the conduction band. This process can be given as [23]

$$O_2+2e^- \rightarrow 2O^-_{ads} \quad (3)$$

This results in the formation of a depletion region near the surface. The depletion region of electrons decreases the electrons concentration in the conduction band of ZnO. Upon exposure to H_2, it readily reacts with the O_2 ions and liberates electrons to the conduction band, accompanied by a decrease in resistance of the films, when it comes in contact with the surface of ZnO:

$$O^-_{ads}+H_2 \rightarrow H_2O+e^- \quad (4)$$

The electrons which are extracted from the conduction band are released to the conduction band of the films, resulting in an increase in number of electrons in the conduction band; subsequently the resistance of the film decreases. Hence, the resistance changes of ZnO film depend on the concentration change of adsorbed oxygen ions on the surface. In addition, MgO phases congregating on the surface of the ZnO particles have influence on the gas sensing properties, due to low electronegativity of Mg (1.31), which can donate electrons to Zn rather than sharing them. Moreover, it does not retard the motion of electron from the conduction band of Zn. So far, the recovery time towards H_2 of 120 s has been rarely reported despite having been achieved using overlayer of MgO on ZnO film.

As significant changes to semiconductor sensors are more likely to occur at low temperature, the sensors were investigated at low temperature up to 225 °C. The variation in response of the ZnO and ZnO/MgO thin film sensors with temperature, upon exposure to 300 sccm of H_2 gas, is shown in Fig. 7. The MgO overlayer influences greatly the response of the sensor towards H_2 as expected. The response increased with increase in temperature, reached a maximum value at about 140 °C for both ZnO and ZnO/MgO films, and then decreased with further increase in temperature. Hence, the optimum operating temperature of the sensor was found to be 140 °C. At 140 °C, the response of ZnO and ZnO/MgO films was observed to be 135 and 260, respectively. The very high response at such a low temperature of the sensor may be associated with the promoting effect of MgO on ZnO. This is because the variation in the response of the sensors upon exposure to reducing gases like H_2 is induced by a modulation of O_2 density in the metal oxides. In the presence of H_2, the ZnO/MgO mixtures give up lattice oxygen to take part in the oxide reaction. The interaction between the ZnO and MgO

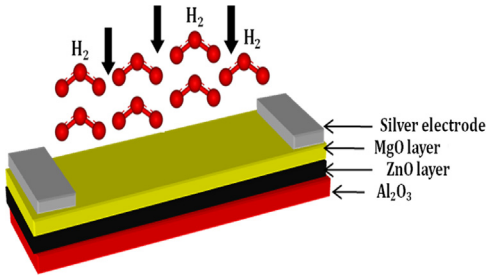

Fig. 5. Schematic representation of the ZnO/MgO sensor device.

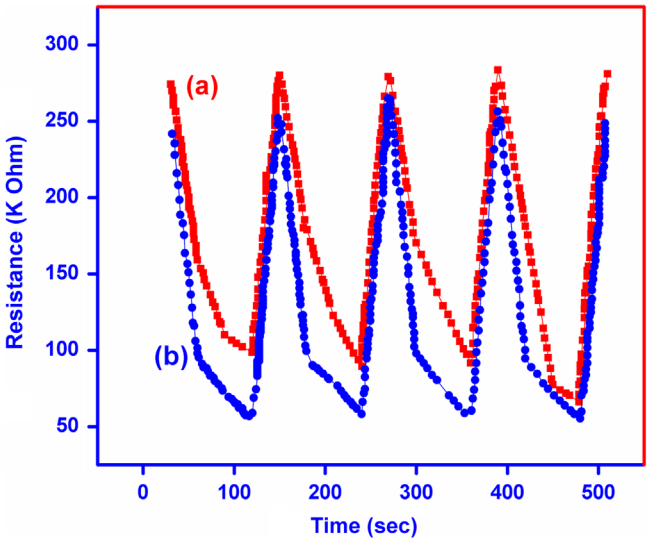

Fig. 6. Response–recovery curves towards H_2 of (a) pure ZnO and (b) ZnO/MgO film with 275 nm thick MgO layer.

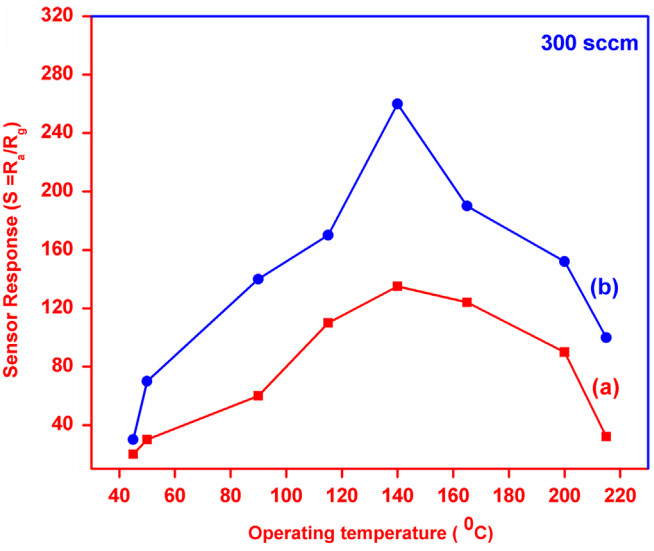

Fig. 7. The variation in sensor response with operating temperature towards H_2 of (a) pure ZnO and (b) ZnO/MgO film with 275 nm thick MgO layer.

components of the sensor material can promote the evolution of lattice oxygen. Liu et al. have reported that, apart from the chemisorbed oxygen, the surface lattice oxygen plays an important role in the sensing mechanism [25]. The reason behind this is that lattice oxygen can modify the chemisorptions rate by altering the availability of local electrons. This results in a large response for ZnO/MgO sensor. When the H_2 gas is removed the reduced metal oxides can adsorb O_2 from the atmosphere and transform it into lattice oxygen again [25,26]. The observed sensor response of ZnO/MgO film towards H_2 is better than that reported previously for Mg: ZnO film towards H_2 [27]. Using the ZnO model system as an example, this study shows that the surface modification of ZnO employing metal oxide layer is a powerful tool for creating new gas specificities, while retaining the basic sensor material.

4. Conclusion

ZnO/MgO films were prepared on Al_2O_3 (0001) substrate by dc sputtering at room temperature. The influences of thickness of MgO overlayer on the structural, morphological and photoluminescence properties of ZnO films were investigated. XRD studies revealed that the preferentially oriented (002) peak significantly improved with thickness of MgO overlayer on ZnO. The strong UV emission peak of ZnO greatly shifted towards the lower wavelength with increase in thickness of MgO layer, indicating the enhanced quantum confinement effect. The energy bandgap increased from 3.10 eV to 3.69 eV as the thickness of MgO layer was increased, indicating the tunable bandgap of ZnO by MgO. SE-micrographs revealed that MgO overlayer plays an important role in the evolution of the morphological properties of ZnO. For 275 nm thick MgO layer on ZnO, compact granular morphology with nanoflake like structure is observed, which is favorable for sensing application. The ZnO/MgO sensor showed higher sensor response to H_2 than that of pure ZnO at the operating temperature of 140 °C, which can be ascribed to high reactivity efficiency of ZnO/MgO films to H_2. The results suggest that the ZnO/MgO film is an excellent material for a low temperature and highly sensitive H_2 sensor.

Acknowledgments

This work was financially supported by the University Grants Commission (Major Research Project-File no. 40-441/2011), which is gratefully acknowledged. The authors thank SASTRA University, Thanjavur, for providing the experimental facilities.

References

[1] Husam S. Al-Salman, M.J. Abdullah, Fabrication and characterization of ZnO thin film for hydrogen gas sensing prepared by RF-magnetron sputtering, Measurement 46 (2013) 1698.
[2] O. Lupan, G. Chai, L. Chow, Fabrication of ZnO nanorod-based hydrogen gas nanosensor, Microelectronics Journal 38 (2007) 1211.
[3] K. Vijayalakshmi, K. Karthick, D. Gopalakrishna, Influence of annealing on the structural, optical and photoluminescence properties of ZnO thin films for enhanced H_2 sensing application, Ceramics International 39 (2013) 4794.
[4] Y.T. Lim, J.Y. Son, J.-S. Rhee, Vertical ZnO nanorod array as an effective hydrogen gas sensor, Ceramics International 39 (1) (2013) 887.
[5] R. Anandhi, R. Mohan, K. Swaminathan, K. Ravichandran, Influence of aging time of the starting solution on the physical properties of fluorine doped zinc oxide films deposited by a simplified spray pyrolysis technique, Superlattices and Microstructures 51 (5) (2012) 680.
[6] Woong Lee, Min-Chang Jeong, Jae-Min Myoung, Catalyst-free growth of ZnO nanowires by metal–organic chemical vapour deposition (MOCVD) and thermal evaporation, Acta Materialia 52 (13) (2004) 3949.
[7] Huo Bingzhi, Hu Lizhong, Zhang Heqiu, Zhao Ziwen, Fu Qiang, Chen Xi, ZnO/MgO distributed Bragg reflectors, Optica Applicata 39 (1) (2009) 169.
[8] Kai Huang, Zhen Tang, Li Zhang, Jiangyin Yu, Jianguo Lv, Xiansong Liu, Feng Liu, Transparent conductive p-type lithium-doped nickel oxide thin films deposited by pulsed plasma deposition, Applied Surface Science 258 (2012) 3710.

[9] Haixia Chen, Jijun Ding, Shuyi Ma, Structural and optical properties of ZnO:Mg thin films grown under different oxygen partial pressures, Physica E 42 (2010) 1487–1491.
[10] P. Bhattacharya, Rasmi R. Das, Ram S. Katiyar, Comparative study of Mg doped ZnO and multilayer ZnO/MgO thin films, Thin Solid films 447 (2004) 564–567.
[11] Amanpal Singha, D. Kumar, P.K. Khanna, Anuj Kumar, Mukesh Kumar, Dielectric anomaly in Mg doped ZnO thin film deposited by sol–gel method, Journal of the Electrochemical Society 158 (1) (2011) G9.
[12] H. Ryu, B.K. Singh, K.S. Bartwal, M.G. Brik, I.V. Kityk, Novel efficient phosphors on the base of Mg and Zn co-doped $SrTiO_3:Pr^{3+}$, Acta Materialia 56 (3) (2008) 358.
[13] H.Q. Huang, F.J. Liu, J. Sun, J.W. Zhao, Z.F. Hu, Z.J. Li, X.Q. Zhang, Y.S. Wang, Effect of MgO buffer layer thickness on the electrical properties of MgZnO thin film transistors fabricated by plasma assisted molecular beam epitaxy, Applied Surface Science 257 (2011) 10721–10724.
[14] N. Tamaekong, C. Liewhiran, A. Wisitsoraat, S. Phanichphant, Sensing characteristics of flame-spray-made Pt/ZnO thick films as H_2 gas sensor, Sensors 9 (2009) 96652–96669.
[15] K. Vijayalakshmi, K. Karthick, Influence of annealing on the photoluminescence of nanocrystalline ZnO synthesized by microwave processing, Philosophical Magazine Letters 92 (2012) 710–717.
[16] S. Suwanboon, P. Amornpitoksuk, A. Sukolrat, Synthesis, characterization and optical properties of $Zn_{1-x}Ti_xO$ nanoparticles prepared via a high-energy ball milling technique, Ceramics International 37 (2011) 1359–1365.
[17] S.J. Chen, Y.C. Liu, J.G. Ma, Y.M. Lu, Zhang, D.Z. Shen, X.W. Fan, Influence of annealing temperature on the structural, optical and mechanical properties of ALD-derived ZnO thin films, Journal of Crystal Growth 254 (2003) 86–91.
[18] Linards Skuja, The origin of the intrinsic 1.9 eV luminescence band in glassy SiO_2, Journal of Non-Crystalline Solids 239 (1998) 16–48.
[19] X.M. Teng, H.T. Fan, S.S. Pan, C. Ye, G.H. Li, Photoluminescence of ZnO thin films on Si substrate with and without ITO buffer layer, Journal of Physics D: Applied Physics 39 (2006) 471–476.
[20] Ruijin Hong, Hongji Qia, Jianbing Huang, Hongbo He, Zhengxiu Fan, Jianda Shao, Influence of oxygen partial pressure on the structure and photoluminescence of direct current reactive magnetron sputtering ZnO thin films, Thin Solid Films 473 (2005) 58–62.
[21] S. Tirpathi, R. Brajpuriya, A. Sharma, A. Soni, G.S. Okram, S.M. Chaudhari, T. Shripathi, Thickness dependent structural, electronic, and optical properties of Ge nanostructures, Journal of Nanoscience and Nanotechnology 8 (2008) 2955.
[22] Y. Tian, H.B. Lu, J.C. Li, Y. Wu, Q. Fu, Synthesis, characterization and photoluminescence properties of ZnO hexagonal pyramids by the thermal evaporation method, Physica E 43 (2012) 410.
[23] S. Choopun, R.D. Vispute, W. Yang, R.P. Sharma, T. Venkatesan, Realization of band gap above 5.0 eV in metastable cubic-phase $Mg_xZn_{1-x}O$ alloy films, Applied Physics Letters 80 (9) (2002) 1529.
[24] K. Patel, W. Clegg, R.M. Pickard, Optimisation of overlay properties for use in magnetic bubble devices, Journal of Physics D: Applied Physics 11 (1978) 531.
[25] Z.X. Liu, Kai Xie, Yu Qing Li, Qi Xun Bao, Behavior of lattice oxygen in V_2O_5/MoO_3 mixture and catalyst, Journal of Catalysis 119 (1) (1989) 249.
[26] P.D. Skafidas, D.S. Vlachos, J.N. Avaritsiotis, Modelling and simulation of abnormal behavior of thick-film tin oxide gas sensors, Sensors and Actuators B 21 (2) (1994) 109–121.
[27] Yanxia Liu, Tao Hang, Yizhu Xie, Zhong Bao, Jie Song, Hongliang Zhang, Erqing Xie, Effect of Mg doping on the hydrogen-sensing characteristics of ZnO thin films, Sensors and Actuators B 160 (2011) 266–270.